

LA-UR- 08-5220

Approved for public release;
distribution is unlimited.

Title: Pressure-induced valence change in YbAl₃ : A combined high pressure inelastic x-ray scattering and theoretical investigation

Author(s): Ravhi S Kumar, Axel Svane, G. Vaitheeswaran, V. Kanchana, Eric D. Bauer, Michael Hu, Malcolm F. Nicol and Andrew L Cornelius

Intended for: Physical Review B



Los Alamos National Laboratory, an affirmative action/equal opportunity employer, is operated by the Los Alamos National Security, LLC for the National Nuclear Security Administration of the U.S. Department of Energy under contract DE-AC52-06NA25396. By acceptance of this article, the publisher recognizes that the U.S. Government retains a nonexclusive, royalty-free license to publish or reproduce the published form of this contribution, or to allow others to do so, for U.S. Government purposes. Los Alamos National Laboratory requests that the publisher identify this article as work performed under the auspices of the U.S. Department of Energy. Los Alamos National Laboratory strongly supports academic freedom and a researcher's right to publish; as an institution, however, the Laboratory does not endorse the viewpoint of a publication or guarantee its technical correctness.

Pressure-induced valence change in YbAl_3 : A combined high pressure inelastic x-ray scattering and theoretical investigation

Ravhi S Kumar¹, Axel Svane², G. Vaitheeswaran³, V. Kanchana³, Eric D. Bauer⁴,

Michael Hu⁵, Malcolm F. Nicol¹ and Andrew L Cornelius¹

¹HIPSEC and Department of Physics and Astronomy, University of Nevada Las Vegas,
Nevada 89154

² Department of Physics and Astronomy, University of Aarhus, Aarhus C, Denmark

³ Applied Materials Physics, Department of Materials Science and Engineering,
Royal Institute of Technology, Brinellvägen 23, 100 44 Stockholm, Sweden

⁴ Los Alamos National Laboratory, New Mexico, USA

⁵ HPCAT, Carnegie Institution of Washington, Advanced Photon Source, Argonne, USA

High resolution x-ray absorption (XAS) experiments in the partial fluorescence yield mode (PFY) and resonant inelastic x-ray emission (RXES) measurements under pressure were performed on the intermediate valence compound YbAl_3 up to 38 GPa. The results of the Yb L_3 PFY-XAS and RXES studies show a smooth valence increase in YbAl_3 from 2.75 to 2.93 at ambient to 38 GPa. *In-situ* angle dispersive synchrotron high pressure x-ray diffraction experiments carried out using a diamond cell at room temperature to study the equation of state showed the ambient cubic phase stable up to 40 GPa. The results obtained from self-interaction corrected local spin density functional calculations to understand the pressure effect on the Yb valence and compressibility are in good agreement with the experimental results.

71.20.Eh, 71.27.+a, 31.15.Ew, 64.30.+t, 62.50.+p

1. INTRODUCTION

Valence fluctuation is a spectacular phenomenon in many rare earth and actinide systems associated with heavy fermion behavior, the Kondo effect, unconventional superconductivity, and volume collapse transitions.^{1,2,3,4} The effect arises due to strong intra-atomic correlations within the f electron manifold of the atoms, which enforces an atomic-like or localized behavior, as opposed to the Bloch-like itinerant picture of electron waves appropriate for normal metallic states in solids. When two quasi-atomic configurations f^n and f^{n+1} become nearly degenerate as a consequence of the chemical environment, the interaction with the conduction electrons leads to a ground state given as a superposition of both configurations. A wealth of phenomenology arises due to the interplay between the energy scales associated with Kondo coupling, the magnetic interatomic exchange interactions and the crystal field effects, the relative strengths of which may be manipulated by external controls like pressure.^{5,6,7,8,9} Hence, high pressure studies are powerful techniques for investigating valence fluctuation phenomena, which is the subject of the present work. Specifically, we explore by experiment and theory the valence fluctuating compound YbAl_3 at high pressure.

YbAl_3 is an intermediate valence compound and exhibits a high Kondo temperature $T_K \sim 670$ K.^{10,11} It has a magnetic susceptibility which follows a Curie-Weiss behavior above 250 K corresponding to an effective magnetic moment of $4.5 \mu_B$.¹² This is indicative of fluctuating atomic-like ($\text{Yb } f^{13}$) local moments at high temperature. The electronic specific heat is large, $58 \text{ mJ mol}^{-1}\text{K}^{-2}$.¹³ YbAl_3 finds application as a thermoelectric material with a large Seebeck co-efficient of $\sim -90 \mu\text{VK}^{-1}$ and a high electrical power factor.¹⁴ Several aspects of the low temperature Fermi liquid coherence

and the cross over to the local moment regime have been studied by transport¹⁵, inelastic nuclear scattering¹⁶, and Lu substitution.¹⁶ However, to extract direct information about the effective Yb valence, high energy spectroscopic techniques, such as Mössbauer, x-ray absorption or high resolution photoemission (PES) experiments must be invoked.^{17,18,19}

Recently, RXES has emerged as an effective tool to probe the mixed valent systems in which the process involves selective enhancement of different valence transitions by choosing appropriate incident energies.²⁰ This technique in conjunction with pressure is an excellent method to study the pressure induced valence changes of rare earth systems and has been applied to a variety of rare earth intermetallic compounds in the past few years.^{21,22} In this paper we describe the investigation of valence changes in YbAl_3 using x-ray absorption spectroscopy (XAS) in the partial fluorescence yield (PFY) mode as well as resonant inelastic x-ray emission studies performed up to 40 GPa. In addition we have performed high pressure x-ray diffraction to determine the equation of state. Theoretical calculations have been carried out for YbAl_3 using the self-interaction corrected local spin-density (SIC-LSD) method. This is an ab-initio electronic structure method, which allows for an accurate, albeit approximate, description of the cohesive properties of the intermediate valence state. The method has previously been applied for a range of Yb compounds, successfully accounting for the trends in observed Yb valences.²³

The paper is organized as follows: in Section II we present our experimental and theoretical methodology, while results of experiment and theory are presented and discussed in Section III. Finally, Section IV concludes the present work.

II. METHODS

a. Experimental

Single crystals of YbAl_3 crystals were grown in Al flux as described elsewhere.¹⁵ The crystals were crushed into fine powder in an agate mortar and powder x-ray diffraction analysis revealed a single phase for the resultant product. The powdered sample was loaded into a 135 μm hole drilled in a Be gasket with few tiny ruby chips and silicone fluid pressure transmitting medium. High pressures were generated using a UNLV- designed three post panoramic type diamond anvil cell employing 300 μm culet diamonds. The x-ray emission spectroscopic data were collected at Sector 16 ID-D of the Advanced Photon Source by focusing the incident x-ray beam to $20 \times 50 \mu\text{m}^2$ (V \times H). The PFY and RXES experiments were performed at the Yb L₃ absorption edge where the signal from the sample was analyzed by a spherically bent Si single crystal and an Amp Tek detector in a Rowland circle. The total energy resolution in our experiments is 1eV.

High pressure x-ray diffraction experiments were performed at Sector 16 ID-B of the Advanced Photon Source in the angle dispersive geometry. The sample was introduced into a 135 μm hole of Re gasket pre-indented to 50 μm and pressurized using a Mao-Bell type diamond anvil cell. We have used poly dimethyl siloxane (silicone fluid) and ruby chips as pressure medium and pressure marker respectively. Diffraction images were collected using a MAR-345 imaging plate up to 40 GPa and integrated using Fit2D software.²⁴ The spectra were further analyzed using the Rietveld (Reitica) package.²⁵

b. Theoretical

The cohesive properties of YbAl_3 are computed with the SIC-LSD method^{26, 27, 28}. This method is based on density functional theory,²⁹ i.e. it relies on a total energy functional by which the energy of the electron sub-system may be calculated at given nuclear positions. The single electron states are determined from solution of a Schrödinger equation with an effective potential, which depends self-consistently on the total charge distribution in the solid. Compared to more conventional approaches, like the LSD, the SIC-LSD method includes a correction for the spurious self-interaction of individual electrons.²⁸ This term favors the formation of spatially localized states as compared to extended Bloch waves, and provides a viable scheme for calculation of cohesive properties of rare earth compounds.^{30, 31} In Yb compounds the method opens up the possibility to describe a mixed valent state by either localizing all 14 f-electrons or localizing 13 f-electrons but allowing the 14th f-electron to hybridize and form bands. The SIC-LSD method evaluates the total energy of the solid in both scenarios, and comparison establishes the appropriate ground state configuration.²³ The divalent configuration of Yb is represented by localizing all 14 f electrons, while the purely trivalent state occurs with 13 localized f-states in the case that the band of the 14th f electron is situated above the Fermi level. The effective valence of Yb in the intermediate valence state follows from the degree of filling of the band of the 14th f electron. If the filling of the band is x , it implies that the wave function may be decomposed into an Yb f^{14} component with probability x and an Yb f^{13} component with probability $1-x$. Hence, this band filling is directly comparable to effective valences derived from experimental

spectra, which involve distinct additive spectra from either of the two Yb configurations f^{13} and f^{14} , as is the case for XAS-PFY and RXES. Technical details of the present implementation can be found in Reference [26].

III. RESULTS AND DISCUSSION

A. Partial Fluorescence Yield and Resonant X-ray Emission

The pressure dependence of the Yb L₃ edge absorption data of YbAl₃ up to 38 GPa is shown in Fig.1. The spectral intensity of 2+ and 3+ contributions at each pressure is calculated by assuming each spectrum as a combination of divalent and trivalent components. The line shape of the trivalent and divalent components was fitted as described earlier.³² PFY-XAS spectra of pure Yb metal and Yb₂O₃ were collected at ambient conditions and served as standards for comparing the 2+ and 3+ intensities and line shapes. The Yb valence in YbAl₃ at each pressure was estimated by substituting the integrated intensities of the 2+ and 3+ components at that pressure into the formula $v = 2 + I_{3+} / [I_{2+} + I_{3+}]$ where I_{2+} and I_{3+} represent 2+ and 3+ intensities, respectively. On analyzing the PFY-XAS ambient spectrum of YbAl₃ we found that the 2+ component resonates for an incident energy $E_{in,2+} = 8.94$ keV, and the 3+ component resonates at a little higher energy, $E_{in,3+} = 8.95$ keV. It is clearly seen that the divalent component, indicated by 2+ in Fig.1, progressively decreases as pressure is increased.

The valence of Yb in YbAl₃ has been studied by different techniques by various groups in the past two decades. While the electrical resistivity experiments performed earlier suggested Yb to possess a nearly trivalent configuration,³³ Mössbauer experiments performed at 1.3 K to 130 K showed no temperature dependence from the observed

isomer shifts and the valence was reported as 2.7.¹⁸ More experiments performed in later years provided further information about the intermediate valence and also its temperature dependence.^{11,34,35,36} We have listed the valence estimated from different techniques in comparison with the current measurements and also listed the calculated valence of Yb at each increasing pressure by PFY-XAS and RXES in Table 1. Even though the Anderson single impurity model reproduces the spectral features reported in the XAS and PES studies quite well, we notice that the valence reported strongly depends on resolution and details of the spectral analysis. In most of the PES measurements the Doniac-Sunjic line shapes were used to estimate the bulk features and the surface contributions were fitted with Gaussian line shapes.^{11,39} High pressure experiments involving the study of valence changes in the heavy fermion compounds are scarce. The mean valence of pure Yb metal has been studied by high pressure x-ray absorption spectroscopy by Syassen *et al.*,³⁷ up to 34 GPa and they reported a continuous valence change from the ambient divalent to the trivalent state above 30 GPa. The valence changes were associated with two structural phase transitions cubic *fcc* to *bcc* at 4 GPa and *bcc* to a *hcp* phase above 30 GPa. PFY-XAS and RXES experiments performed on YbAl₂ recently showed pressure induced valence change from 2.25 at ambient pressure to 2.9 at 38.5 GPa.³² On comparing our PFY-XAS and RXES experimental results with these reports mentioned above we arrive at the following: The valence change in YbAl₃ is sluggish compared to YbAl₂ and is not associated with any structural phase transitions as can be seen from the diffraction results provided in the following section. The RXES spectrum collected at 38 GPa is shown in Fig. 2. The inset (a) in the figure shows the

pressure dependent RXES spectra excited with an incident energy $E_{\text{in}} = 8.938$ keV below the absorption threshold.

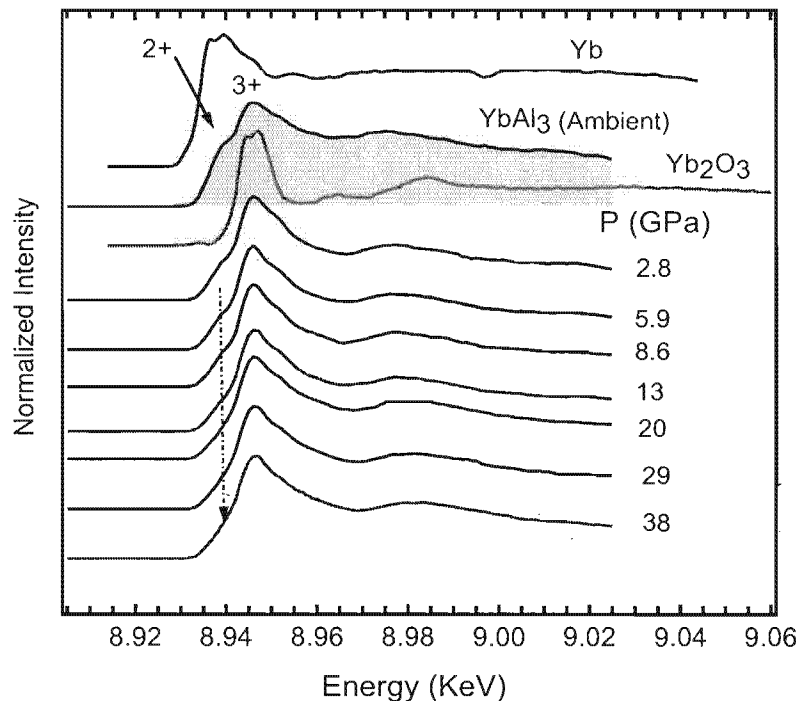


Fig.1. X-ray absorption spectra of YbAl₃ in the PFY mode. The dotted arrow indicates continuous decrease of 2+ component as a function pressure. The XAS spectrum of the YbAl₃ sample at ambient temperature and pressure is shown with Yb and Yb₂O₃ standards.

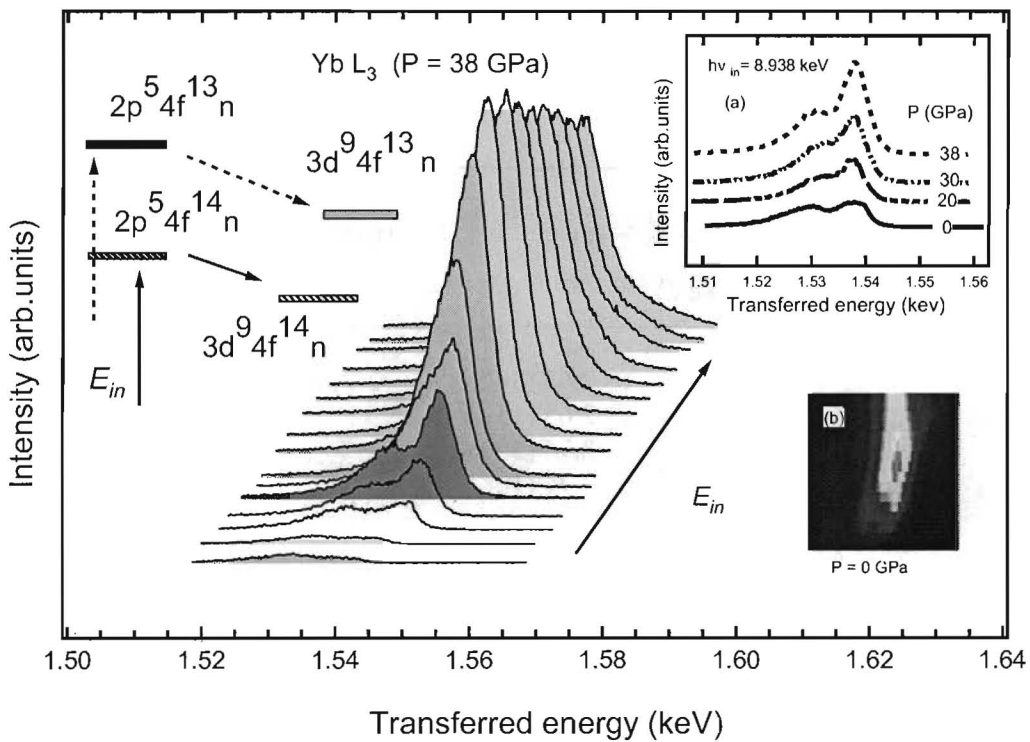


Fig.2 Resonant x-ray emission spectra of YbAl_3 at 38 GPa. The incident energy was scanned in steps of 2 eV. A schematic representation of the transition is shown on the left. The RXES experiments were performed at the L_3 edge of Yb by measuring the $\text{L}\alpha_1$ x-ray emission as a function of pressure with incident energy of 8.945 keV. (a) RXES spectrum with $E_{in} = 8.938$ keV at different pressures and (b) 2D image of the ambient spectrum.

Table 1. Estimated Yb valence in YbAl_3 by various spectroscopic techniques

Pressure (GPa)	PFY-XAS ^a	RXES ^a ($E_{\text{in}} = 8.938$ keV)	PES	HAXPES	XAS	Theory ^a
Ambient	2.75	2.76	2.65 (300K) ^b 2.65 (15K) ^c 2.74 (300K) ^c 2.77 (10K) ^d	2.71 (180K) ^e	2.775 (300K) ^f	2.62
9	2.82	2.83				2.68
20	2.86	2.85				2.72
38	2.93	2.88				2.78

^a present work, ^b Reference³⁸, ^c Reference³⁹, ^d Reference¹¹, ^e Reference⁴⁰, ^f Reference³⁶,

The increasing 3+ contribution is evident from the increase in intensity of the peak around 8.95 keV, which is situated approximately 7 eV above the peak due to the 2+ component. The inset (b) shows the 2D image of the RXES spectrum collected at ambient pressure. The branching of the 2+ and 3+ components is clearly visible. However there is a difference in the valence estimated from the two measurements i.e. PFY-XAS and RXES at $E_{\text{in}} = 8.938$ keV as listed in Table 1. This arises due to the ambiguity in the intensity estimation for the fluorescent peak arising between 2+ and 3+

components as discussed previously for YbAl_2 .³² The pressure dependency of the Yb valence is illustrated in Fig.3.

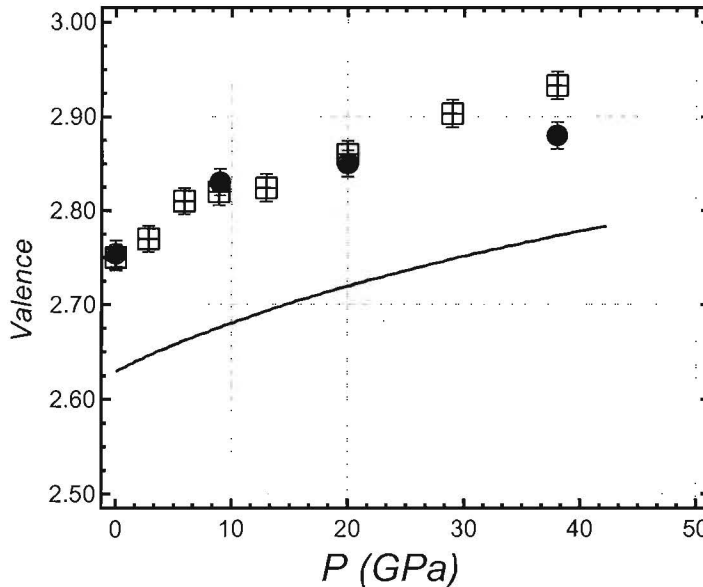


Fig. 3. Valence as a function of pressure for PFY-XAS (squares) and RXES (circles) experiments. The solid line represents theoretical simulation.

The effective valence determined from the SIC-LSD calculations is seen to be approximately 0.13 lower than the experimentally derived, but the observed increase with pressure is well reproduced by the calculations. Given the intricacy of the concept of valence and the theoretical approximations of the SIC-LSD approach the agreement can be considered quite satisfactory.

B. High pressure x-ray diffraction

Diffraction patterns collected at various pressures are shown in Fig. 4. The diffraction pattern collected at the lowest pressure ($P = 3.8$ GPa) in the diamond anvil cell was indexed well with the cubic $Pm-3m$ structure as reported in the literature.⁴¹ The prominent diffraction peaks were monitored continuously on increasing pressure. We have observed no changes in the diffraction pattern except a gradual shift in the diffraction lines as indicated by the dotted lines shown in the spectra.

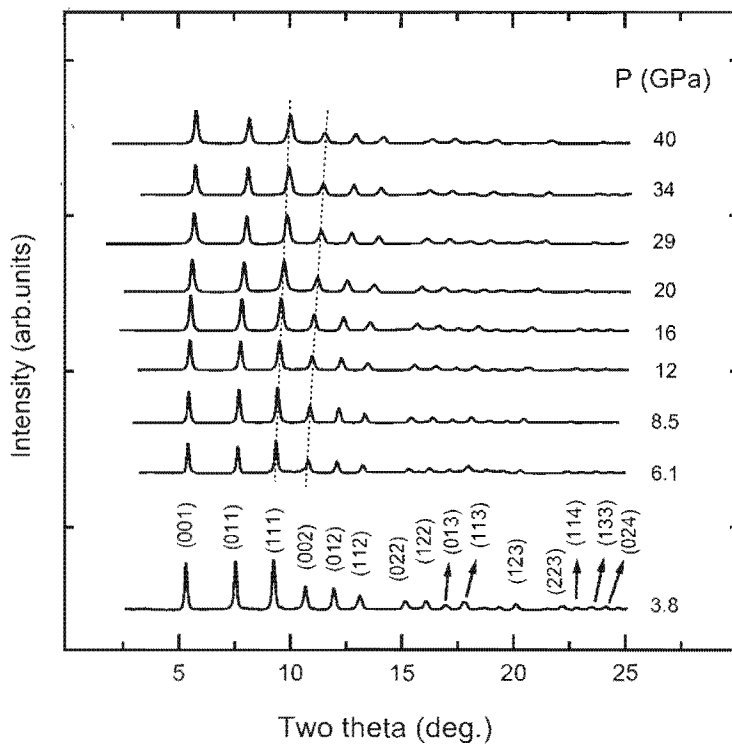


Fig.4. Representative x-ray diffraction patterns at different pressures for YbAl_3 . The dotted lines are guides for the eye, which indicate the shift observed in the diffraction lines on increasing pressure.

No new features were observed in the diffraction patterns except systematic shift of the lines during compression and the compound remained in the cubic structure up to the highest pressure achieved in our experiments. The bulk modulus was computed by fitting the pressure-volume data (Fig.5) to a second order Birch-Murnaghan equation of state. The values of B_0 and B_0' are found to be $B_0 = 65.2(3)$ and $B_0' = 5.6(1)$ respectively. The effect of high pressure on the crystal structure of rare earth trialuminides was comprehensively investigated a long time ago.⁴² Recently RAI_2 and RAI_3 ($\text{R} = \text{La}$ and Ce) type compounds have been studied under pressure up to 30 GPa.⁴³ The bulk modulus obtained for YbAl_3 compares well with the YbAl_2 , LaAl_3 and CeAl_3 compounds as shown in Table 2.

Table 2. Structural properties of YbAl_3 compared to CeAl_3 and LaAl_3 .

Name of compound	Ambient structure and cell parameters (\AA)	Bulk modulus (B_0) GPa	Pressure derivative (B_0')	Reference
YbAl_3	Cubic, $Pm-3m$ $a = 4.2125(2)$ $a = 4.108$	65.2(3) 92.3	5.6(1)	expt. (this work) theory (this work)
CeAl_3	Hexagonal, $P6_3/mmc$ $a = 6.541(5)$ $c = 4.610(3)$	41(3)	6.7(2)	Ref. 43
LaAl_3	Hexagonal, $P6_3/mmc$ $a = 6.680(1)$ $c = 4.619(1)$	63(4)	4.0(6)	Ref. 43

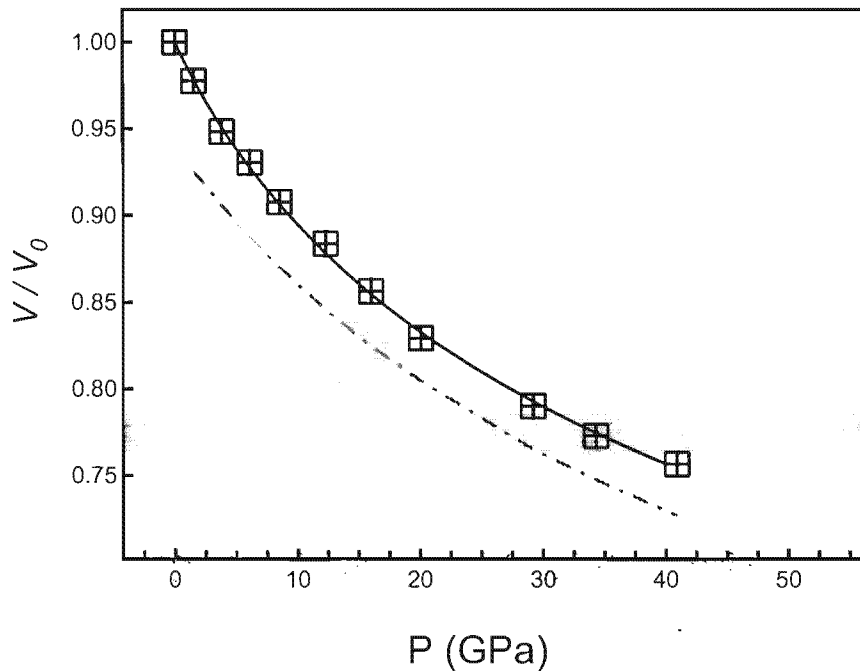


Fig. 5. Pressure-volume relation of YbAl_3 . The solid line is the fit with a second order Birch-Murnaghan equation of state. The dotted line is the theoretical simulation.

However the bulk modulus of YbAl_3 is found to be lower than the calculated bulk modulus values of similar transition metal trialuminides such as ZrAl_3 , HfAl_3 etc. which are used in the high temperature structural applications.⁴⁴

C. Results of calculations

The total energies of YbAl_3 were calculated as a function of volume with the Yb localized configuration taken to be either f^{13} or f^{14} , as outlined in section IIb. The results are shown in figure 6. For the sampling of the charge density of the conduction electrons the calculations used 32^3 k-points in the full Brillouin zone corresponding to 969 k-points in the irreducible wedge of the Brillouin zone.

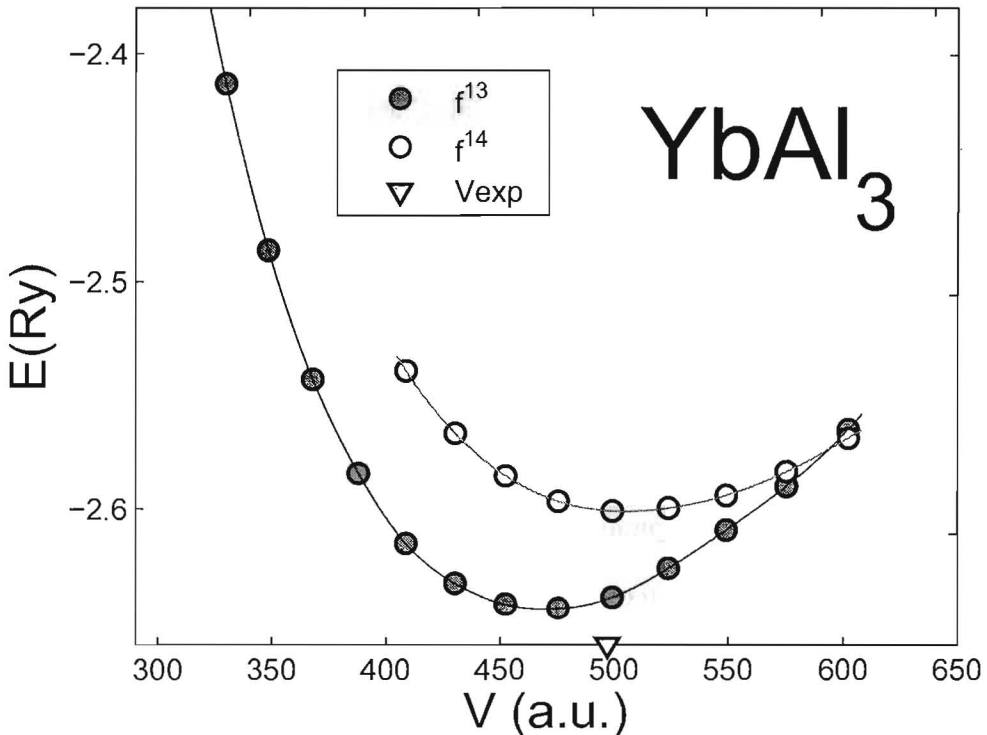


Fig 6. Total energy as a function of volume (per formula unit) for YbAl_3 calculated with the SIC-LSD approach with either 13 (squares) or 14 (circles) localized f electrons. The triangle marks the experimental equilibrium volume.

The ground state of YbAl_3 is found for the intermediate valent state corresponding to 13 localized f electrons in agreement with the experimental observation. The total energy minimum is found at a specific volume of $490 \text{ } a_0^3$, corresponding to a theoretical equilibrium lattice constant of 4.108 \AA . This is 2.2 % smaller than the experimental value of $4.2125(2) \text{ \AA}$ measured in the present work. This discrepancy is a combined effect of the underlying LSD approximation and the geometrical approximations of the present implementation of the SIC-LSD method. The LSD is well known to generally underestimate bond length.⁴⁵ The geometrical approximations of the present scheme involve the so-called atomic spheres approximation⁴⁶ (ASA), which in particular for Al is less accurate than a more complete full-potential treatment. For pure Al the lattice constant calculated with the restrictions of the ASA is 1.6 % lower than the value calculated within a full-potential treatment. For Yb, on the other hand, the specific volume calculated within ASA is in perfect agreement with the experimental value.²³

In Figure 5 we compare the theoretical $p(V)$ curve including this deficiency in equilibrium volume to the experimental data. By coincidence, the equilibrium lattice constant for the divalent Yb configuration agrees better with the experimental value, but the energy of this state is found $\sim 0.6 \text{ eV}$ higher than the intermediate valent state (per formula unit), i.e. this configuration is not realizable.

The calculated bulk modulus of YbAl_3 is 92.3 GPa, which is considerably larger (by $\sim 40 \text{ \%}$) than the experimental value of 65.2(3) GPa. The major reason for this is the too small equilibrium volume already discussed which also influences the curvature of the total energy curve with an ensuing drastic influence on the bulk modulus. If evaluated at

the experimental equilibrium volume we find $B(V_{\text{exp}}) = 77 \text{ GPa}$, $B'(V_{\text{exp}}) = 4.3$, these numbers being in considerably better agreement with the experimental values of Table 2.

The calculated effective valence of Yb in YbAl_3 as a function of (calculated) pressure is included in Figure 3 for comparison with the experimental values. The calculated values are seen to be somewhat smaller than the experimentally derived values, by approximately 0.13, however showing the same smoothly increasing behavior with pressure. The effective valency increases by ~ 0.15 as pressure is raised from 0 to 40 GPa, both in experiment and theory.

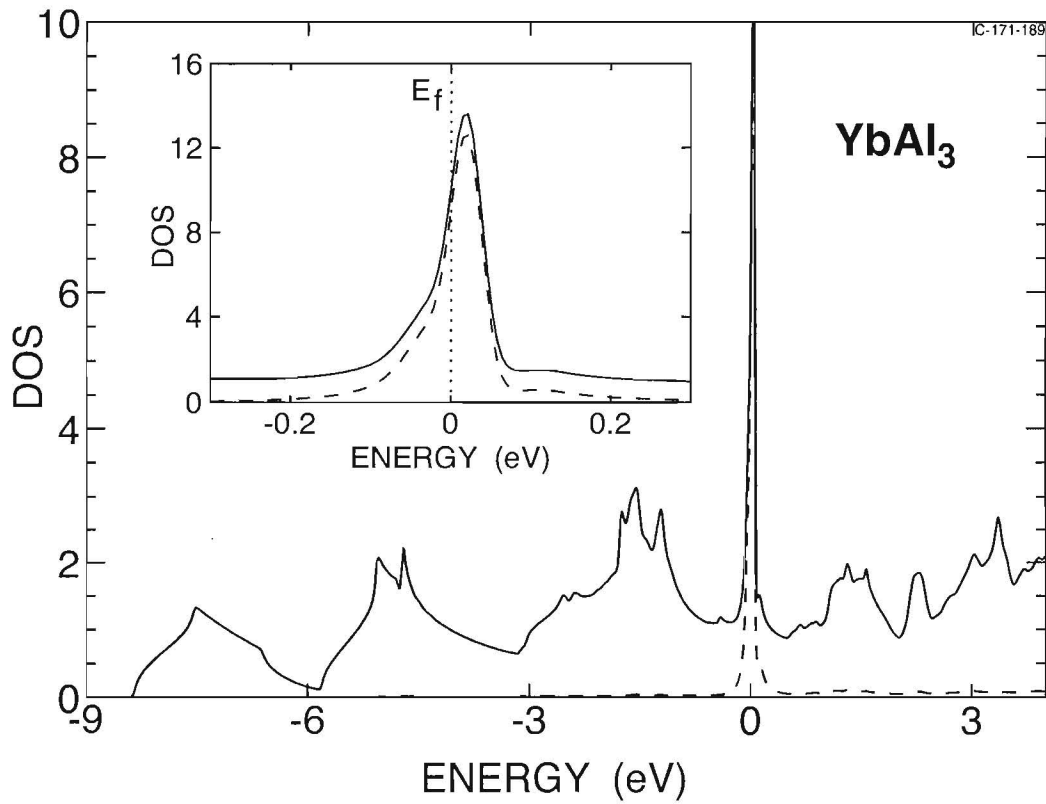


Fig 7. SIC-LSD density of states (dos) for YbAl_3 (units are states per formula unit and per eV). The Fermi energy is at zero energy. Full line is the total dos, while dashed line

gives the Yb f projected dos. The inset shows the region close to the Fermi level, where the partial occupation of the f-resonance is evident. With pressure this resonance moves upward in energy with respect to the Al bands with an ensuing gradual depletion, i.e. Yb approaches the trivalent configuration.

In Figure 7, we show the density of one-electron states calculated for the intermediate valent ground state of YbAl_3 . One notices the Al valence bands ranging from 8.4 eV below the Fermi level and intersected by the narrow f band situated at the Fermi level. The inset shows the region close to the Fermi level and illustrates the partial filling of this band, which determines the effective valence. This density of states is not directly comparable to an experimental photoemission spectrum but merely serves to elucidate, how the SIC-LSD ground state is built from one-particle states. Most notably, the localized states are not shown. A full treatment of photoemission in rare earths need to take into account the atomic character of the f electrons with all multiplet effects of the initial and final states included.⁴⁷

IV. CONCLUSIONS

We have studied the pressure dependence of the effective valence of Yb in the intermediate valence compound YbAl_3 using high resolution PFY-XAS and RXES techniques. High pressure spectra were collected up to 38 GPa. The equation of state of YbAl_3 is further investigated up to 40 GPa using high resolution powder x-ray diffraction. Self-interaction corrected density functional calculations were performed simultaneously in order to compare the experimental results. The pressure dependence of the Yb valence was derived from the experimental data, and showed an increase from

2.75 to 2.93 as pressure is increased from 0 to 38 GPa. This trend compares well with the theoretical investigations.

ACKNOWLEDGEMENTS

Work at UNLV is supported by DOE award No. DEFG36- 05GO08502. HPCAT is a collaboration among the UNLV High Pressure Science and Engineering Center, the Lawrence Livermore National Laboratory, the Geophysical Laboratory of the Carnegie Institution of Washington, and the University of Hawaii at Manoa. The UNLV High Pressure Science and Engineering Center was supported by the U.S. Department of Energy, National Nuclear Security Administration, under Cooperative Agreement No. DE-FC08- 01NV14049. Use of APS was supported by the U.S. Department of Energy, Office of Science, Office of Basic Energy Sciences, under Contract No. W-31-109-ENG-38. G. V and V. K acknowledge V R and SSF for the financial support.

¹ A.C. Hewson, *The Kondo Problem to Heavy Fermions* (Cambridge University Press, Cambridge, 1993).

² J.M. Lawrence, P.S. Riseborough, and R.D. Park, Rep. Prog. Phys. **44**, 3 (1981).

³ T. Kasuya and T. Sasó, *Theory of Heavy Fermions and Valence Fluctuations* (Springer :Berlin, 1985).

⁴ J.W. Allen, S.J. Oh, O. Gunnarsson, K. Schönhammer, M.B. Maple, M.S. Torikachvili, and I. Lindau, Adv. Phys. **35**, 275 (1986).

⁵ E.D. Bauer, R. Hauser, E. Gratz, D. Gignoux, D. Schmitt, and J. Sereni, J. Phys. Condensed Matter **4**, 7829 (1992).

⁶ D. Wohlleben and B. Wittershagen, Adv. Phys. **34**, 1985 (403).

⁷ Y. Kishimoto, Y. Kawasaki, and T. Ohno, Phys. Lett.A **317**, 308 (2003).

⁸ A.V. Goltsev and M.M. Abd-Elmeguid, J. Phys. Condensed Matter **17**, S813 (2005).

⁹ P. Monachesi and A. Continenza, Phys. Rev. B **47**, 14622 (1993).

¹⁰ E.E. Havinga, K.H.J. Buschow, and H.J. van Daal, Solid State Commun. **13**, 621 (1973).

¹¹ L.H. Tjeng, S.-J. Oh, E.-J Cho, H.-J. Lin, C.T. Chen, G.-H. Gweon, J.-H. Park, J.W. Allen, T. Suzuki, M.S. Makivic, and D.L. Cox, Phys. Rev. Lett **71**, 1419 (1993).

¹² K.H.J Buschow, U. Goebel, and E. Dormann, Phys.Stat.Sol.(b) **93**, 607 (1979).

¹³ T. Ebihara, S. Uji, C. Terakura, T. Terashima, E. Yamamoto, Y. Haga, Y. Inada, and Y. Onuki, Physica B **281**, 754 (2000).

¹⁴ D.M. Rowe, V.L. Kuznetsov, L.A. Kuznetsova, and G. Min, J. Phys. D **35**, 2183 (2002).

¹⁵ A.L. Cornelius, J.M. Lawrence, T. Ebihara, P.S. Riseborough, C.H. Booth, M.F. Hundley, P.G. Pagliuso, J.L. Sarrao, J.D. Thompson, M.H. Jung, A.H. Lacerda, and G.H. Kwei, Phys. Rev. Lett **88**, 1172011 (2002).

¹⁶ E.D. Bauer, C.H. Booth, J.M. Lawrence, M.F. Hundley, J.L. Sarrao, J.D. Thompson, P.S. Riseborough, and T. Ebihara, Phys. Rev. B **69**, 125102 (2004).

¹⁷ F. Patthey, J.M. Imer, W.D. Schneider, Y. Baer, B. Delley, and F. Hulliger, Phys. Rev. B **36**, 7697 (1987).

¹⁸ J.J. Joyce, A.B. Andrews, A.J. Arko, R.J. Bartlett, R.I.R Blythe, C.G. Olson, P.J. Benning, P.C. Canfield, and D.M. Poirier, Phys. Rev. B **54**, 17515 (1996).

¹⁹ J.W. Ross and E. Tronc, J. Phys. F **8**, 983 (1978).

²⁰ C. Dallera and M. Grioni, Struc. Chem. **14**, 57 (2003).

²¹ C. Dallera, M. Grioni, A. Shukla, G. Vanko, J.L. Sarrao, J.-P. Rueff, and D. Cox, Phys. Rev. Lett **88**, 196403 (2002).

²² J.-P Rueff, J.-P. Itie, M. Taguchi, C.F. Hague, J.-M. Mariot, R. Delaunay, J.-P. Kappler, and N. Jaouen, Phys. Rev. Lett **96**, 237403 (2006).

²³ W.M. Temmerman, Z. Szotek, A. Svane, P. Strange, H. Winter, A. Delin, B. Johansson, O. Eriksson, L. Fast, and J. Wills, Phys. Rev. Lett. **83**, 3900 (1999); A. Svane, W.M. Temmerman, Z. Szotek, L. Petit, P. Strange, and H. Winter, Phys. Rev. B **62**, 13394 (2000).

²⁴ A.P. Hammersley, S.O. Svensson, M. Hanfland, A.N. Fitch, and D. Hausermann, High Press. Res. **29**, 301 (1996).

²⁵ C.J. Howard and B. Hunter (*unpublished*).

²⁶ A. Svane, Phys.Rev.B **53**, 4275 (1996).

²⁷ W.M. Temmerman, A. Svane, Z. Szotek, H. Winter and S. Beiden in *Electronic structure and physical properties of solids: The uses of the LMTO method*, Lecture Notes in Physics, Vol.535, edited by H. Dreysee (Springer Verlag, Berlin 2000), pp. 286-312.

²⁸ J.P. Perdew and A. Zunger, Phys.Rev.B **23**, 5048 (1981).

²⁹ P. Hohenberg and W. Kohn, Phys.Rev. **136**, B864 (1964).

³⁰ P. Strange, A. Svane, W.M. Timmerman, Z. Szotek, and H. Winter, Nature (London) **399**, 756 (1999).

³¹ A. Svane, W.M. Temmerman, Z. Szotek, L. Petit, P. Strange, and H. Winter, Phys.Rev.B **62**, 13394 (2000); G Vaitheeswaran, L. Petit, A. Svane, V. Kanchana, and M. Rajagopalan, J.Phys.C **16**, 4429 (2004); A. Svane, V. Kanchana, G. Vaitheeswaran, G. Santi, W.M. Temmerman, Z. Szotek, P. Strange, and L. Petit, Phys.Rev.B **71**, 045119 (2005); A. Svane, G. Santi, Z. Szotek, W.M. Temmerman, P. Strange, M. Horne, G. Vaitheeswaran, V. Kanchana, and L. Petit, Phys.Stat.Sol. (b) **241**, 3185 (2004).

³² C. Dallera, E. Annese, J.-P Rueff, A. Palenzona, A. Vanko, L. Braicovich, A. Shukla, and M. Grioni, Phys .Rev. B **68**, 245114 (2003).

³³ E.E. Havinga, K.H.J. Buschow, and H.J. van Daal, Sol.State.Commun. **13**, 621 (1973).

³⁴ E-J. Cho, S.-J. Cho, C.G. Olson, J.-S. Kang, R.O. Anderson, L.Z. Liu, J.H. Park, and J.W. Allen, Physica B **186-188**, 70 (1993).

³⁵ S. Suga, A. Sekiyama, S. Imada, A. Shigemoto, A. Yamasaki, M. Tsuenekawa, C. Dallera, L. Braicovich, T.-L. Lee, O. Sakai, T. Ebihara, and Y. Onuki, J. Phys. Soc. Jpn. **74**, 2880 (2005).

³⁶ J.M. Lawrence, G.H. Kwei, P.C. Canfield, J.G. Dewitt, and A.C. Lawson, Phys. Rev. B **49**, 1627 (1994).

³⁷ K. Syassen, G. Wortmann, J. Feldhaus, K.H. Frank, and G. Kaindl, Phys. Rev. B **49**, 1627 (1994).

³⁸ En-Jin Cho, J.-S. Chung, S.-J. Oh, S. Suga, M. Taniguchi, A. Kakizaki, A. Fujimori, H. Kato, T. Miyahara, T. Suzuki, and T. Kasuya, Phys. Rev. B **47**, 3933 (1993).

³⁹ S.-J. Oh, Physica B **186-188**, 26 (1993).

⁴⁰ A. Sekiyama and S. Suga, J. Elect. Spect. and Rel. Phen., **137-140**, 681 (2004).

⁴¹ A. Palenzona, J. Less Comm. Metals **29**, 289 (1972).

⁴² J.F. Cannon and H. Tracy Hall, J. Less. Comm. Metals **40**, 313 (1975).

⁴³ M. Sekar, N.V. Chandra Shekar, P.Ch. Sahu, N.R. Sanjay Kumar, and K. Govinda Rajan, Physica B **324**, 240 (2002).

⁴⁴ C. Colinet and A. Pasturel, J. Alloys and Compds. **319**, 154 (2001).

⁴⁵ R.O. Jones and O. Gunnarsson, Rev. Mod. Phys. **61**, 689 (1989).

⁴⁶ O.K. Anderson, Phys. Rev. B, **12**, 3060 (1975).

⁴⁷ S. Lebegue, G. Santi, A. Svane, O. Bengone, M.I. Katsnelson, A.I. Lichtenstein, and O. Eriksson, Phys. Rev. B, **72**, 245102 (2005).